Transport in Porous Media **46:** 77–89, 2002.

Non-linear Model for Wood Saturation

STEFAN JAN KOWALSKI[1], GRZEGORZ MUSIELAK[1] and LESŁAW KYZIOŁ[2]

[1]*Institute of Technology and Chemical Engineering, Poznań University of Technology, pl. Marii Skłodowskiej-Curie 2, 60-965 Poznań, Poland. e-mail: stefan.j.kowalski@put.poznan.pl; Grzegorz.Musielak@put.poznan.pl*

[2]*Institute of Shipboard Machinery Fundamentals, ul. Śmidowicza 71, 81-919 Gdynia, Poland. e-mail: lkyz@amw.gdynia.pl*

(Received: 25 July 2000; in final form: 20 April 2001)

Abstract. The paper presents a non-linear model of saturation with fluid of anisotropic capillary porous bodies and the results of experimental investigations of wood saturation with methacrylate. The obtained experimental curves illustrating the distribution of methacrylate in wood samples allow the estimation of material coefficients and verification of the theoretical model. The theoretical model is developed based on the balance equations of mass, momentum, and energy, and the thermodynamics of irreversible processes. The non-linear differential equation, describing the distribution of methacrylate content in wood and its evolution during the saturation is solved numerically. The theoretical curves obtained on the basis of both linear and non-linear models are compared with the experimental data and better agreement between them for the non-linear model is stated.

Key words: wood saturation, non-linear and linear models, experimental tests, results comparison.

1. Introduction

The aim of the paper is to develop a theoretical model of saturation with fluids of anisotropic capillary porous bodies and to present the results of experimental investigations of wood saturation with methacrylate. The elaborated theoretical model enables the control of the amount of saturating substance (here: methacrylate), adsorbed by wood in a given interval of time. It can be helpful by wood modification with various substances for the purpose of improvement of its physical properties such as increase of wood strength, hardness, or reduction of wood humid sorption ability. The control of saturation is necessary to obtain required wood properties, which depend evidently on the amount of adsorbed substance as well as on its distribution in wood.

The experimental tests of wood saturation with methacrylate of methyl group were carried out for estimation of the coefficients appearing in the theoretical model and comparison of the theoretical and experimental results.

There are a number of contributions dealing with saturation of wood. For example, the capillary-porous model of wood structure and the influence of wood internal structure on liquid transport were studied by Siau (1984, 1985, 1995).

Mathematical models of water soaking wood were presented in Rosen (1974a,b) and Olek (1997). The mechanical behaviour of water soaked wood at various states of stress was examined experimentally in Kowal *et al.* (1992), Kowal and Kowalski (1995). The physical relations for wood at variable humidity were published in Ranta-Maunus (1975), Bazant (1985), and Kowalski and Kowal (1998), Kowalski and Musielak (1999).

The present theoretical model differentiates from those presented in the above papers with the mechanism of mass transport in the pore space. Namely, one assumes here that the gradient of a generalised chemical potential of the fluid (dependent on the thermodynamical state) is the main thermodynamical force responsible for the fluid transport in wood. The generalised chemical potential includes the capillary and gravitational potentials.

The experimental tests were carried out on pine sapwood and pine hardwood. The saturation substance in both cases was the methacrylate of methyl group and the saturation process was led separately in the radial and tangential directions with respect to the annual wood rings. The amount of absorbed mass and its distribution were measured in the cross-section of the tested bar and also calculated numerically using the elaborated model. In conclusion, one states that the non-linear theoretical predictions reflect qualitatively better experimental results than the results obtained on the basis of linear theory.

2. Derivation of the Theoretical Model

Let us assume that the saturated wood consist of two components: wood fibres (skeleton) and liquid in pores. Unsaturated (dry) wood is characterised by bulk mass density ρ^{s} [kg/m^3], and the fluid in pores by bulk mass density ρ^{f} [kg/m^3]. The notion 'bulk' means that the above mentioned masses are referred to the same representative volume element (RVE) of wood. The porosity ϕ is defined as the ratio of pore volume to the volume of the RVE. The volumetric saturation S is the fraction of pore space filled with liquid. The mass saturation of wood θ is defined as the mass of fluid referred to the mass of unsaturated wood, that is

$$\theta = \frac{\rho^{\mathrm{f}}}{\rho^{\mathrm{s}}} = S\frac{\rho^{\mathrm{rf}}\phi}{\rho^{\mathrm{s}}}, \tag{1}$$

where ρ^{rf} denote the real mass density of fluid.

Wood is generally a deformable body. The mass balances for dry wood and fluid in pores read as

$$\dot{\rho}^{\mathrm{s}} = -\rho^{\mathrm{s}}\dot{\varepsilon}, \tag{2}$$

$$\rho^{\mathrm{s}}\dot{\theta} = -\mathrm{div}\,\mathbf{w}, \tag{3}$$

where ε is the volumetric strain of wood and $\mathbf{w}$ denotes the fluid mass flux (efflux or influx). Dot over a symbol denotes the substantial derivative with the velocity of solid network as the convection velocity.

Writing balance of energy, we take into account both mechanical and thermal interactions between wood fibres and the fluid in pores. In this paper, however, the attention will be focused mainly on the saturation process and not on wood deformation.

Let $u = u^{\mathrm{s}} + \theta u^{\mathrm{f}}$ be the internal energy of saturated wood referred to the mass of dry wood. Time alteration of the internal energy is due to mechanical work of stresses on the wood strains, and due to heat supply, that is

$$\rho^{\mathrm{s}}\dot{u}u = \sigma_{ij}\dot{\varepsilon}_{ij}\varepsilon_{ij} - (q_i + h^{\mathrm{f}}w_i),_i + w_i g_i + R. \tag{4}$$

In the above formula: σ_{ij} and ε_{ij} are the stress and strain tensors, g_i, q_i and w_i denote the gravity acceleration and the heat and the fluid mass fluxes, h^{f} and R are the fluid enthalpy and the volumetric heat supply, and $(-),_i \equiv \partial(-)/\partial x_i$ denotes differentiation with respect to spatial derivative.

If wood is brought to contact with fluid, the process of saturation proceeds automatically. That means that it is a self-acting process similarly to the conduction of heat. Thus, we consider the thermal and saturation processes to be irreversible, and this means that these processes cause an increase of entropy.

Let $s = s^{\mathrm{s}} + \theta s^{\mathrm{f}}$ be the entropy of saturated wood referred to the mass of dry wood. The variation of this entropy in time reads

$$\rho^{\mathrm{s}}\dot{s} = \rho^{s}\dot{s}_{\mathrm{int}} - \left(\frac{q_i}{T} + w_i s^{\mathrm{f}}\right),_i + \frac{R}{T}. \tag{5}$$

The new symbols in the above formula are: s_{int} the entropy production during the irreversible process, s^{f} the specific entropy of fluid, T the absolute temperature.

The volumetric heat supply R is an *a priori* defined quantity. Separating this quantity from balance of energy (4) and substituting it into balance of entropy (5), one gets the second law of thermodynamics in the form of the following inequality

$$\begin{aligned}\rho^{\mathrm{s}}\dot{s}_{\mathrm{int}} \;=\; & \frac{\rho^{\mathrm{s}}}{T}\left[-(\dot{f} + s\dot{T}) + \frac{1}{\rho^{\mathrm{s}}}\sigma_{ij}\dot{\varepsilon}_{ij} + \mu^{\mathrm{f}}\dot{\theta}\right] - \\ & - \left[\frac{1}{T}w_i(\mu^{\mathrm{f}},_i - g_i) + \frac{1}{T^2}(q_i + w_i s^{\mathrm{f}}T)T,_i\right] \geqslant 0,\end{aligned} \tag{6}$$

where $f = u - sT$ is the free energy, and $\mu^{\mathrm{f}} = h^{\mathrm{f}} - s^{\mathrm{f}}T$ is the free specific enthalpy (chemical potential of fluid).

Formula (6) has to be satisfied for both reversible and irreversible processes. For reversible processes no fluxes occur and the entropy production is equal to zero. Formula (6) in this case is reduced to

$$\dot{f} = -s\dot{T} + \frac{1}{\rho^{\mathrm{s}}}\sigma_{ij}\dot{\varepsilon}_{ij} + \mu^{\mathrm{f}}\dot{\theta}. \tag{7}$$

We identify Equation (7) as Gibbs' identity for saturated porous solid. It indicates that the time alteration of the free energy is due to the time alteration of

temperature, strain tensor, and fluid content in pores. In present considerations, we will assume that Gibbs' identity in its form (7) obeys also for quasi-static processes, that is, processes proceeding close to the thermodynamic equilibrium. Substituting (7) into (6) one obtains the residual inequality of the form

$$-\left[w_i(\mu^{\mathrm{f}},_i - g_i) + \frac{1}{T}(q_i + w_i s^{\mathrm{f}} T)T,_i \right] \geqslant 0. \tag{8}$$

As the main aim of this paper is to develop the model for wood saturation in isothermal conditions, we confine further considerations to derivation of mass transfer equation. Then, we assume the temperature gradient to be zero, that is $T,_i = 0$. By this assumption the inequality (8) will be satisfied if

$$w_i = -K_{ij}(\mu^{\mathrm{f}},_j - g_j), \tag{9}$$

where K_{ij} are the coefficients of a positively defined quadratic form which will be created when substituting (9) into (8) (with $T,_i = 0$).

Having in mind Equation (7), we conclude that the free energy depends on the temperature, strain tensor, and fluid content. These quantities are taken to be the parameters of state. The chemical potential has to be also a function of state depending on the same parameters of state as the free energy, that is

$$\mu^{\mathrm{f}} = \left(\frac{\partial f}{\partial \theta}\right)_{\varepsilon,T} = \mu^{\mathrm{f}}(T, \varepsilon_{ij}, \theta) = f^{\mathrm{f}} + \frac{p^{\mathrm{f}}}{\rho^{\mathrm{fr}}}. \tag{10}$$

If we take into account that the pressure p^{f} of the pore fluid differs from the pressure p_0 (= const) of free fluid by capillary pressure p^{cap}, we can split the chemical potential into the standard potential $\mu(p_0, T) = f^{\mathrm{f}} + p_0/\rho^{\mathrm{fr}} = \overset{\circ}{\mu}(T)$ (see Prigogine and Defay, 1954) and the capillary potential μ^{cap}

$$\mu^{\mathrm{f}}(T, \varepsilon_{ij}, \theta) = \overset{\circ}{\mu}(T) + \mu^{\mathrm{cap}}(t, \varepsilon_{ij}, \theta). \tag{11}$$

The capillary potential is defined as the capillary pressure divided by the real fluid density ρ^{rf}

$$\mu^{\mathrm{cap}}(T, \varepsilon_{ij}, \theta) = \frac{p^{\mathrm{cap}}(T, \varepsilon_{ij}, \theta)}{\rho^{\mathrm{rf}}}. \tag{12}$$

The capillary pressure, on the other hand, can be expressed as a function of saturation (see e.g., Scheidegger, 1957; Cairncross *et al.*, 1996). Having in mind the shape of this function given in theses papers we have constructed the following relation between the capillary pressure in i-direction and the saturation

$$(p^{\mathrm{cap}})_{(i)} = -A_{(i)} \frac{\gamma}{\sqrt{k_{(i)}}} \frac{1 - S}{S + \sqrt{\phi}}, \quad 0 \leqslant S \leqslant 1, \tag{13}$$

where constants $A_{(i)}$ were chosen on the base of experimental data obtained by authors (details are given in the next section). New terms in this formula are: the

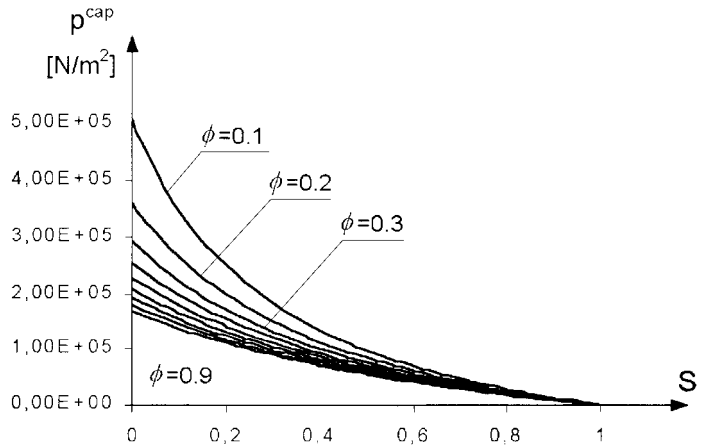

Figure 1. Capillary pressure versus volumetric saturation $S = \theta\rho^{\mathrm{s}}/\rho^{\mathrm{rf}}\phi$.

surface tension γ (generally dependent on the temperature), the permeability in i-direction $k_{(i)}$ and the porosity ϕ. Note that

$$S = \theta\frac{\rho^{\mathrm{s}}}{\rho^{\mathrm{rf}}\phi} \quad \text{and} \quad \phi = \phi_0 + (1-\phi_0)\varepsilon, \tag{13a}$$

where ϕ_0 is the porosity of wood in the reference configuration, and $\varepsilon = \varepsilon_{xx}+\varepsilon_{yy}+\varepsilon_{zz}$ denotes the volumetric strain. Thus, the capillary pressure depends indirectly on the parameters of state, that is $p_{\mathrm{cap}} = p_{\mathrm{cap}}(T, \varepsilon, \theta)$. Graphical performance of the capillary pressure function is presented in Figure 1.

The permeability for wood depends on spatial orientation: crosswise (radial (R) and tangential (T) to the growth rings), or longitudinal (L) to the natural wood fibres. The capillary potential is dependent on permeability, so it differs for the above mentioned directions.

One can imagine wood as being consisting of three kinds of capillary pipes of different diameter situated perpendicularly to each other (orthotropy). Using the well-known Hagen–Poiseuille solution for the flow of liquid having viscosity η in a pipe, one estimates coefficients K_{ij} in the rate Equation (9) as follows:

$$[K_{ij}] = \begin{bmatrix} K_{(L)} & 0 & 0 \\ 0 & K_{(R)} & 0 \\ 0 & 0 & K_{(T)} \end{bmatrix} \quad \text{where} \quad K_{(i)} = \phi\frac{k_{(i)}}{\eta}(\rho^{\mathrm{rf}})^2. \tag{14}$$

If the gradient of strain is assumed to be negligibly small, what is usually true by free saturation, then the gradient of potential μ^{f} for the isothermal case (T = const) reads

$$\mu^{\mathrm{f}}{}_{,i} \approx \left(\frac{\partial\mu^{\mathrm{cap}}}{\partial\theta}\right)_{\varepsilon,T}\theta_{,i} = \frac{1}{\rho^{\mathrm{rf}}}\left(\frac{\partial p^{\mathrm{cap}}}{\partial\theta}\right)_{\varepsilon,T}\theta_{,i} = \frac{1}{\rho^{\mathrm{rf}}}\left(\frac{\partial p^{\mathrm{cap}}}{\partial S}\right)_{\varepsilon,T}S_{,i}\,. \tag{15}$$

Substituting (14) and (15) into (9) and next into (3) one obtains

$$\dot{S} = \frac{k_{(i)}}{\eta}\left[\left(\frac{\partial p^{\mathrm{cap}}}{\partial S}\right)_{\varepsilon,T} S_{,i}\right]_{,i} . \tag{16}$$

Note: indices in brackets (i) do not involved the Einstein summation rule! The structural and physical parameters $(\phi, k_{(i)}, \rho^{\mathrm{s}}, \rho^{\mathrm{rf}}, \eta)$ are assumed to be constant in further considerations. Thus, the above formula can be written as follows:

$$\dot{S} = \Lambda_{(i)}\left[\frac{1}{(S+\sqrt{\phi})^2} S_{,i}\right]_{,i} \quad \text{where} \quad \Lambda_{(i)} = A_{(i)}\left(1+\sqrt{\phi}\right)\sqrt{k_{(i)}}\frac{\gamma}{\eta}. \tag{17}$$

Equation (17) is used in this paper for calculations of the amount of fluid content and its distribution in the tested wood.

3. Experimental Programme

The experimental investigation of wood saturated with methacrylate was carried out in a special autoclave in vacuum conditions. The wood under investigation was pine sapwood and pine hardwood. The sapwood and hardwood timbers of rectangular cross-section 40×75 mm were cut out in parallel to wood fibres from a log having the diameter of 350 mm and the length of 3000 mm. The timbers were subjected to drying and seasoning in the laboratory conditions. Their average moisture content after seasoning was ca. 8%.

The rectangular samples of dimension $40 \times 75 \times 100$ mm (see Figure 2) were made of the square timbers. They had no defects like knots, decay or insect injury. The dimensions of 18 samples made of sapwood and 18 samples made of sapwood were: in radial direction 40 mm, tangential direction 75 mm and lengthwise direction 100 mm. The dimensions of other 18 samples made of sapwood and 18 samples made of sapwood were: in radial direction 75 mm, tangential direction 40 mm and lengthwise direction 100 mm. 72 samples were prepared. The surfaces of dimensions 40×100 mm and 40×75 mm were isolated in each sample with chlorinated enamel and resin. The soaking surfaces were those of 75×100 mm.

The samples were dried, numbered and weighed first, followed by the saturation with the methacrylate in the autoclave. Six periods of saturation were realised: 4, 25, 100, 250, 400, and 800 h. In each test four samples were saturated at once: two samples made of sapwood and two samples made of hardwood, among them one prepared for radial and one prepared for tangential saturation. Each saturation process was repeated three times, so: 4 (samples in one test) $\times$ 3 (test's repeat) $\times$ 6 (saturation periods) $=$ 72 samples.

After saturation process, four rectangular prisms of dimensions $40 \times 20 \times 20$ mm were cut out from the middle part of each saturated sample (see Figure 2(c)), and at once put in the polyurethane foil to preserve their saturation for longer

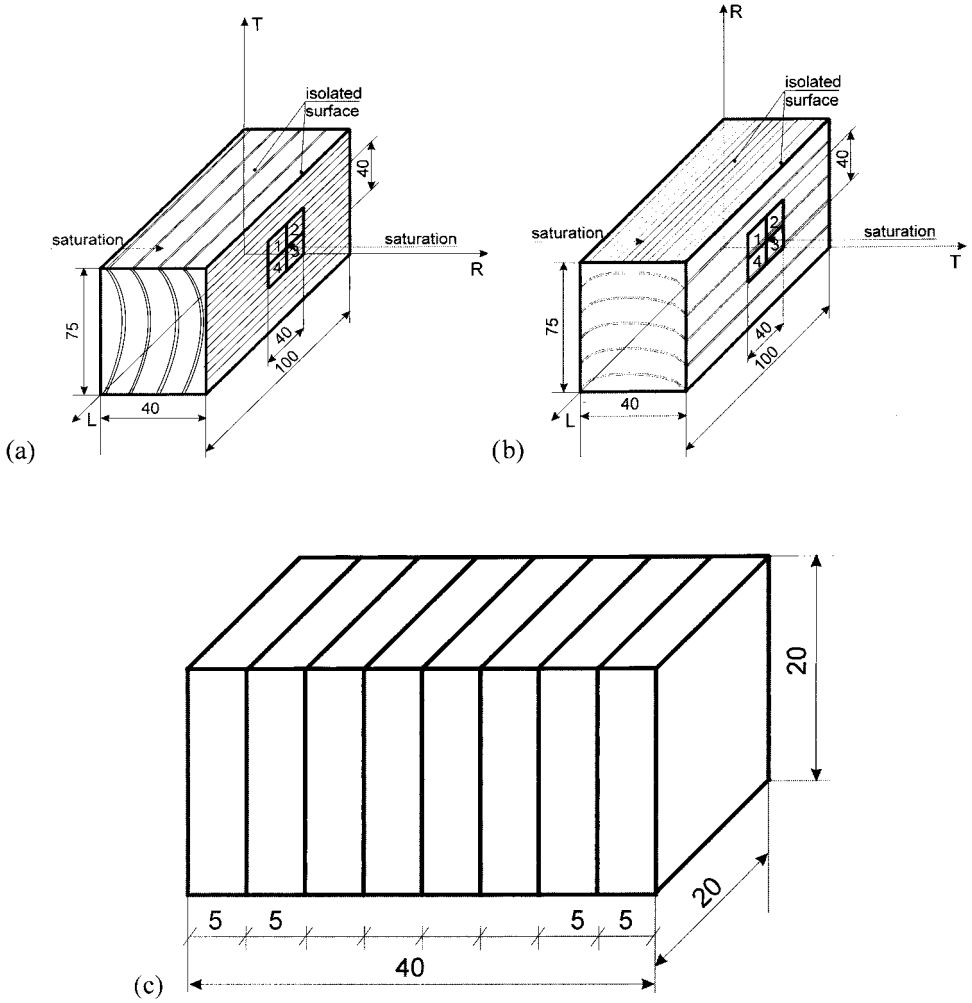

Figure 2. Wood samples: (a) saturation in radial direction, (b) saturation in tangential direction, (c) rectangular prism.

time. The prisms were next cut into 5 mm slices along the length of 40 mm, eight slices were obtained together from each prism. Every slice was weighted and next dried until the weight of each slice did not change any more. During this drying the methacrylate was removed totally from wood samples. That means that polymerisation of methacrylate did not proceed in the tested samples.

Figure 3 presents the distributions of methacrylate in sapwood and hardwood by saturation in radial and tangential directions for six different periods of saturation. The experimentally determined distributions of the methacrylate content are drawn as piece-wise horizontal lines. Each horizontal line expresses the average value of methacrylate content in the individual section.

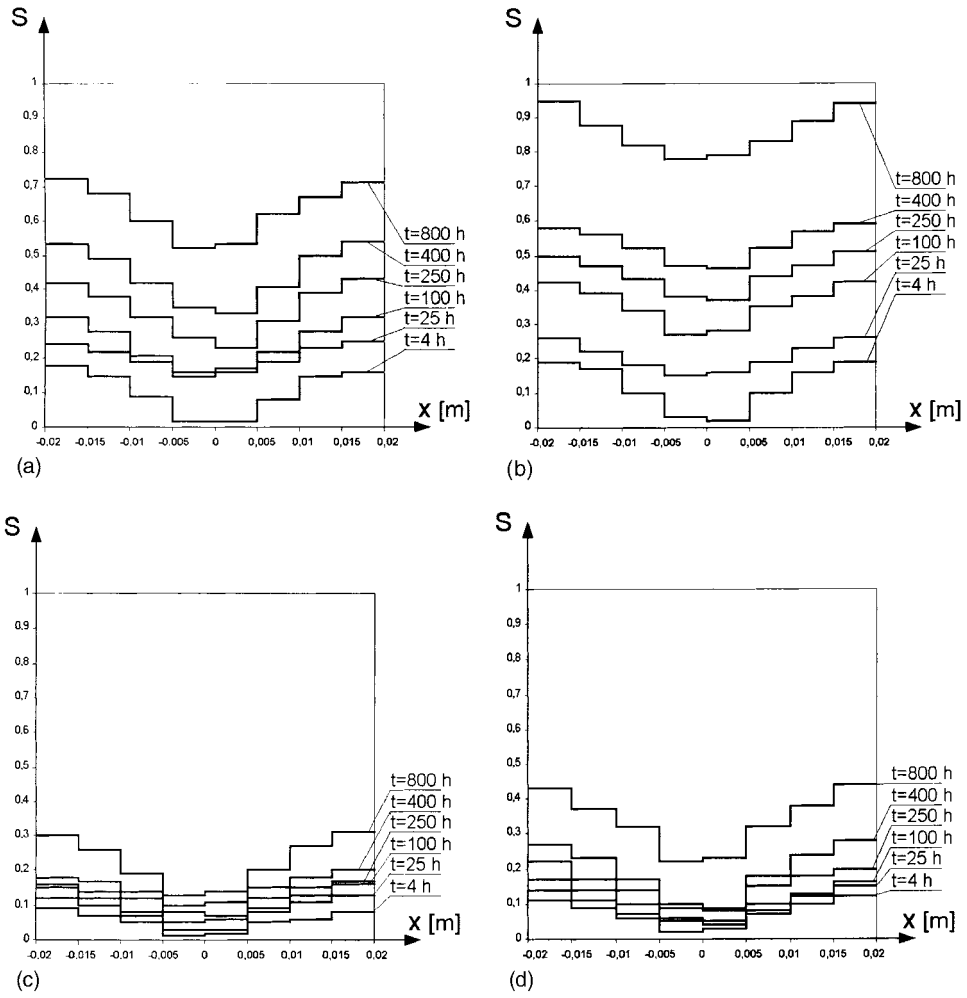

Figure 3. Distribution of methacrylate in wood samples: (a) sapwood saturated in radial direction, (b) sapwood saturated in tangential direction, (c) hardwood saturated in radial direction, (d) hardwood saturated in tangential direction.

Figure 4 presents the rate of saturation of the individual sections of sapwood and hardwood saturated both in radial and tangential directions.

The results obtained experimentally confirm the common knowledge that saturation proceed easier in sapwood than in hardwood and is more intensive in tangential than in radial direction. The data obtained in experimental tests give the possibility of estimation of the coefficients in the mathematical model, and in particular the constant $A_{(i)}$ in the formula (13) for capillary pressure and α_m in boundary condition (19).

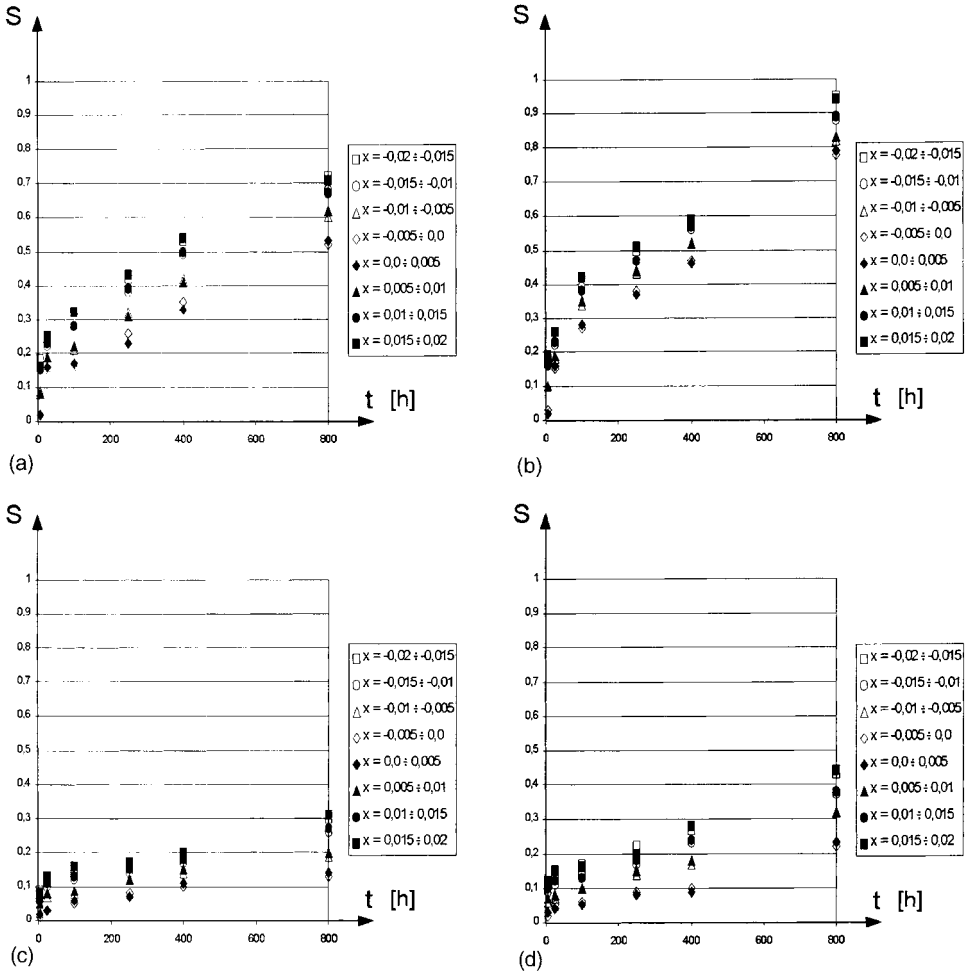

Figure 4. Saturation rate in individual sections of the sample: (a) sapwood saturated in radial direction, (b) sapwood saturated in tangential direction, (c) hardwood saturated in radial direction, (d) hardwood saturated in tangential direction.

4. Initial-Boundary Value Problem

Having in mind the rectangular prisms of 40 mm in length and square cross-section of 20×20 mm cut out from the middle part of the saturated sample (see Figure 2(c)), we assume that the saturation of such a prism was one-dimensional. We assume then, that the distribution of the methacrylate is uniform in a cross-section of the prism and that the problem is symmetrical with respect to the middle plane of the prism of 40 mm in length. The symmetry follows from the identical saturation of the sample's sides.

The initial-boundary value problem was solved numerically using the non-linear and linear models, for comparison. We formulate the non-linear initial-boundary

value problem as follows: find the distribution of methacrylate concentration $S(x, t)$ in the rectangular prism and its evolution in time using Equation (17) at zero initial concentration and the following boundary conditions

$$\frac{\partial S}{\partial x} = 0 \quad \text{for} \quad x = 0, \tag{18}$$

$$-\Lambda_{(i)} \frac{\rho^{\mathrm{f}}}{(S + \sqrt{\phi})^2} S_{,i} = \alpha_m (1 - S) \quad \text{for} \quad x = \pm L, \tag{19}$$

where $\Lambda_{(i)}$ is the coefficient stimulating the rate of saturation, and α_m expresses the intensity of saturation at the boundary. These boundary conditions describe mass fluxes. The condition (18) states that the mass flux through the plane of symmetry equals zero. The left hand side of (19) denotes the fluid flux on the boundary inside (see Equations (9), (14) and (15)), and the right hand side denotes the fluid flux on the boundary outside. The condition (19) expresses the fact that the saturation gradient is maximal at the beginning of the saturation process, that is when $S = 0$, and decreases in the course of saturation. When the boundary is fully saturated, $S = 1$, the fluid flux is equal to zero.

The methacrylate of methyl group is characterised by the following parameters: surface tension $\gamma = 28.1 \times 10^{-3}$ N/m, viscosity $\eta = 0.569 \times 10^{-3}$ Pa·s, wetting angle $\cos\alpha = 0.989$, mass density $\rho^{\mathrm{rf}} \equiv \rho^m = 945\,\mathrm{kg/m^3}$, boiling point $T = 374$ K. The mass density of dry pine sapwood $\rho^{\mathrm{s}} = 567\,\mathrm{kg/m^3}$, the porosity $\phi = 0.68$, the permeability in directions: radial $k_{(R)} = 6 \times 10^{-17}\,\mathrm{m^2}$ and tangential $k_{(T)} = 4 \times 10^{-16}\,\mathrm{m^2}$.

For the linear model, instead of Equation (17) and boundary condition (19), the following equations are applied:

$$\dot{S} = \Lambda_{(i)} S_{,ii} \quad \text{where} \quad \Lambda_{(i)} = A_{(i)} \left(1 + \sqrt{\phi}\right) \sqrt{k_{(i)}} \frac{\gamma}{\eta}, \tag{20}$$

with boundary condition (18), and the following one:

$$-\Lambda_{(i)} S_{,i} = \alpha_m (1 - S) \quad \text{for} \quad x = \pm L, \tag{21}$$

instead of (19). The coefficients $A_{(i)}$ and α_m were estimated on the basis of experimental data and the optimisation procedure. The difference between the experimental data and the theoretical solutions was minimised according to the following quadratic norm N

$$N = \sum_{i=1}^{8} \sum_{j=1}^{6} (\hat{S}_{ij} - \tilde{S}_{ij})^2, \tag{22}$$

where $\hat{S}_{ij}$ is the set of experimental data for i-th section and time $t_j = \{4, 25, 100, 250, 400 \text{ and } 800\,\mathrm{h}\}$, and

$$\tilde{S}_{ij} = \int_{x_i}^{x_{i+1}} S(x, t_j)\,\mathrm{d}x, \tag{23}$$

is the average value of saturation in i-th section obtained theoretically. Here $x_i = \{-0.02; -0.015; -0.01; -0.005; 0.00; 0.005; 0.01; 0.015; 0.02\,\mathrm{m}\}$.

Minimum of the norm N was sought by making use of the combination of the Monte Carlo and the genetic algorithm methods. The pair of material coefficients $\{A_{(i)}, \alpha_m\}$ is chosen to be the specimen for 'play'. First, a subset of specimens is chosen randomly from the possible values of material coefficients ('first generation'). The quality of each specimen is proved by the norm N. Next, the best pair of specimens ('parents') is chosen from the 'first generation' and a new set of specimens ('second generation') is created. The quality of each element of the 'second generation' is proved. If an element of better quality than that of the previously chosen 'parents' is found, then the 'parents' are replaced by this new element. The procedure is repeated up to that moment until the required convergence is reached. For example, for the pine sapwood saturated in radial direction it was founded $A_{(i)} = 0.51 \times 10^{-7}$ and $\alpha_m = 0.525 \times 10^{-3}$ as the best chosen values of material coefficients.

The non-linear differential Equation (17) was solved numerically by making use of the finite difference method – explicit scheme (see e.g., Potter, 1982). Half of the rectangular prism of dimension 20 mm was divided into 100 equal elements. The time step was taken 0.1 s, and this value was sufficient to guarantee the stability of numerical procedure. The non-linear boundary conditions (18) and (19) were approximated by 20 iterations in each step. As a result of these calculations the function $S(x, t)$ was found. Its value was evidently dependent on the material coefficients.

The linear problem, equations (20), (18) and (21), was solved precisely according to the procedure suitable for the well-known Sturm–Liouville problem. The final integral of the linear problem takes the form

$$S(x,t) = 1 - \sum_{n=0}^{\infty} \frac{4\alpha_m \cos \omega_n L}{\omega_n \Lambda_{(i)}(2\omega_n L + \sin 2\omega_n L)} \exp(-\omega_n^2 \Lambda_{(i)} t) \cos \omega_n x, \quad (24)$$

where the periodic numbers are determined from the following characteristic equation

$$\operatorname{tg} \omega L = -\frac{\alpha_m}{\omega \Lambda_{(i)}}. \quad (25)$$

5. Comparison of Experimental and Theoretical Curves

The distributions of methacrylate content in the samples of pine sapwood and hardwood, saturated in radial and tangential directions, were determined experimentaly for six different periods of saturation. We have decided not to calculate numerically all theoretical curves of methacrylate distribution, adequate to experimental ones, because they are quantitatively similar to each other, and the numerical calculations take a lot of time. Therefore, we shall present only some representative theoretical curves illustrating distribution of methacrylate in pine sapwood saturated in radial

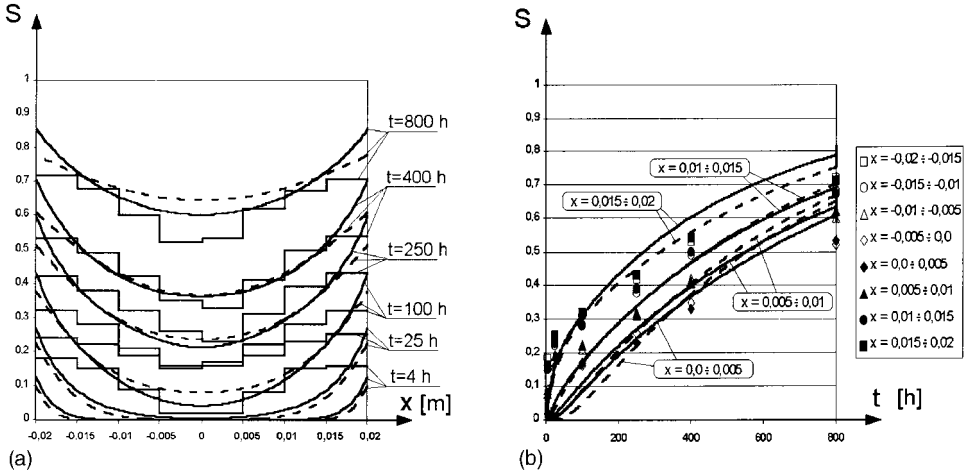

Figure 5. (a) Distribution of methacrylate in sapwood samples saturated in radial direction: experiment – stepped line; non-linear theory – solid line; linear theory – broken line. (b) Rate of saturation of the individual prisms of the sapwood sample: experiment – points; non-linear theory – solid line; linear theory – broken line.

direction for six periods of saturation, and the rate of saturation of several sections of the prism presented in Figure 2(c).

The results are presented in Figure 5. The experimental data are drawn as piecewise horizontal lines. Each horizontal line expresses the average value of the methacrylate content in individual section. The solid curves express the theoretically predicted methacrylate content distributions calculated on the basis of non-linear Equation (17). The doted lines illustrate the theoretical solution (24), based on the linear model. One can state that the non-linear model better approximate the experimental data than the linear one, in particular those for the long periods of saturation. The accuracy of fitting of the experimental and theoretical data (expressed by the norm N) is $N = 0.3796$ for the non-linear model, while for the linear one $N = 0.4584$. The accuracy of the non-linear model depends heavily on the shape of the capillary pressure function.

The theoretical curves well reflect the experimental data as far as it concerns the general tendency. There are, however, some discrepancies in their quantitative agreement. The reason is, as usual, in difficulties of repeatability of experimental measurements.

6. Final Remarks

The main goal of this work was to find out a theoretical model of saturation of anisotropic capillary-porous materials for the purpose of controlled saturation of wood with methacrylate and other substances. The distribution of the saturating substance in wood and its evolution in time is described by a non-linear differential equation of diffusive type. The non-linearity appears because of the application of

the capillary potential as the main force responsible for the mass transport in wood pores. In the linear model the mass flux is proportional to the gradient of volumetric saturation.

The theoretical curves well reflect qualitatively the experimental tendency, however, quantitatively some discrepancies for some curves are visible. The discrepancies are even much greater for the linear model of saturation. The numerical results show that the non-linear model much better predict the experimental data than the linear one.

Acknowledgement

Part of this work has been financially supported by the research project DS 32/013/2001, realised at Poznań University of Technology.

References

1. Bazant, Z. P.: 1984, Constitutive equation of wood at variable humidity and temperature, *Wood Sci. Technol*. **19**, 159–177.
2. Cairncross, R. A., Schunk, P. R., Chen, K. S., Prakash, S. S., Samuel, J., Hurd, A. J. et al.: 1996, Drying in deformable partially-saturated porous media: sol-gel coatings, Sandia Report – 2149, UC-905.
3. Kowal, M., Rybarczyk, W. and Kowalski, S. J.: 1992, Mechanical behaviour of water soaked wood at various states of stress, *Wood Sci.Technol*. **26**, 295–306.
4. Kowal, M. and Kowalski, S. J.: 1995, Experimental investigation of water soaked wood at uniaxial and biaxial state of stress, *Appl. Mech. Rev*. **48**, 684–688.
5. Kowalski, S. J. and Kowal, M.: 1998, Physical relation for wood at variable humidity, *Transport in Porous Media* **31**, 331–346.
6. Kowalski. S. J. and Musielak, G.: 1999, Deformation and stresses in dried wood, *Transport in Porous Media* **34**, 239–248.
7. Musielak, G.: 1996, Internal stresses caused by outflow of moisture and phase change inside dried material, *Drying Technology* **14**, 289–306.
8. Olek, W.: 1997, Modelling of sorption process of water in coniferous wood, *PhD at Agriculture Academy Poznań*.
9. Potter, D.: 1982, *Numerical Methods of Physics, Computer Physics*, PWN-Warszawa, (in Polish).
10. Prigogine, I. and Defay, R.: 1954, *Chemical Thermodynamics*, Longman Green and Co, London, New York, Toronto.
11. Ranta-Maunus, A.: 1975, The viscoelasticity of wood at varying moisture content, *Wood Sci. Technol.* **9**, 189–205.
12. Rosen, H. N.: 1974a, Penetration of water into hardwood, *Wood Fiber* **5**, 275–287.
13. Rosen, H. N.: 1974b, Distribution of water in hardwoods: a mathematical model, *Wood Sci. Technol.* **8**, 283–299.
14. Scheidegger, A. E.: 1957, *The Physics of Flow Through Porous Media*, University of Toronto Press, Toronto.
15. Siau, J. F.: 1984, *Transport Processes in Wood*, Springer-Verlag, Berlin.
16. Siau, J. F.: 1985, Nonisothermal moisture diffusion experiments analysed by four alternative equations, *Wood Sci. Technol.* **19**, 151–157.
17. Siau, J. F.: 1995, *Wood: Influence of Moisture on Physical Properties*, Virginia Tech., Blacksburg.